Anomaly of oxygen bond-bending mode at 320 cm^{-1} and additional absorption peak in the *c*-axis infrared conductivity of underdoped $YBa_2Cu_3O_{7-\delta}$ single crystals revisited with ellipsometric measurements

C. Bernhard
Max-Planck-Institut für Festkörperforschung, Heisenbergstrasse 1, D-70569 Stuttgart, Germany

D. Munzar
Max-Planck-Institut für Festkörperforschung, Heisenbergstrasse 1, D-70569 Stuttgart, Germany and Department of Solid State Physics and Laboratory of Thin Films and Nanostructures, Faculty of Science, Masaryk University, Kotlářská 2, CZ-61137 Brno, Czech Republic

A. Golnik* and C. T. Lin
Max-Planck-Institut für Festkörperforschung, Heisenbergstrasse 1, D-70569 Stuttgart, Germany

A. Wittlin
Institute of Physics, Polish Academy of Sciences, Aleja Lótnikow 32, PL-02-668, Poland

J. Humlíček
Department of Solid State Physics and Laboratory of Thin Films and Nanostructures, Faculty of Science, Masaryk University, Kotlářská 2, CZ-61137 Brno, Czech Republic

M. Cardona
Max-Planck-Institut für Festkörperforschung, Heisenbergstrasse 1, D-70569 Stuttgart, Germany

(Received 26 July 1999)

We have performed ellipsometric measurements of the far-infrared *c*-axis dielectric response of underdoped $YBa_2Cu_3O_{7-\delta}$ single crystals. Here we report a detailed analysis of the temperature-dependent renormalization of the oxygen bending phonon mode at 320 cm^{-1} and the formation of the additional absorption peak around 400–500 cm^{-1}. For a strongly underdoped $YBa_2Cu_3O_{6.5}$ crystal with $T_c=52$ K we find that, in agreement with previous reports based on conventional reflection measurements, the gradual onset of both features occurs well above T_c at $T^*\sim 150$ K. Contrary to some of these reports, however, our data establish that the phonon anomaly and the formation of the additional peak exhibit very pronounced and steep changes right at T_c. For a less underdoped $YBa_2Cu_3O_{6.75}$ crystal with $T_c=80$ K, the onset temperature of the phonon anomaly almost coincides with T_c. Also in contrast to some previous reports, we find for both crystals that a sizeable fraction of the spectral weight of the additional absorption peak cannot be accounted for by the spectral-weight loss of the phonon modes but instead arises from a redistribution of the electronic continuum. Our ellipsometric data are consistent with a model where the bilayer cuprate compounds are treated as a superlattice of intrabilayer and interbilayer Josephson junctions.

I. INTRODUCTION

It was early recognized that some of the infrared active *c*-axis phonon modes of the high-T_c cuprate superconductors exhibit rather strong changes (so-called ''phonon anomalies'') in the vicinity of the superconducting transition.[1] The most pronounced phonon anomalies have been observed for those compounds that contain two (or three) closely spaced CuO_2 layers per unit cell, like the bilayer compounds $YBa_2Cu_3O_{7-\delta}$ (Y-123),[2,3] $YBa_2Cu_4O_8$ (Y-124),[4] and $Pb_2Sr_2CaCu_2O_8$,[5] or the trilayer system $Tl_2Ba_2Ca_2Cu_3O_{10}$.[6] In Y-123 and Y-124 the most pronounced renormalization occurs for the so-called oxygen bond-bending mode at 320 cm^{-1}, which involves the in-phase vibration of the O(2) and O(3) oxygen ions of the CuO_2 planes against the Y ion that is located in the center of the bilayer and against the ions of the CuO chains.[7] The renormalization of the 320-cm^{-1} mode is accompanied by the formation of an additional broad absorption peak in the frequency range between 400 and 500 cm^{-1} at low temperature. The effects are most spectacular for strongly underdoped $YBa_2Cu_3O_{6.5-6.6}$ with $T_c\sim 50$–60 K. Here the phonon mode at 320 cm^{-1} softens by almost 20 cm^{-1} and loses most of its spectral weight which is transferred to the additional broad peak. As the hole doping of the CuO_2 planes increases, the anomaly of the 320-cm^{-1} phonon mode becomes less pronounced. Simultaneously, the additional peak shifts towards higher frequencies and becomes considerably weaker.

Evidently, there exists an intimate relationship between the strong anomaly of the oxygen bond-bending mode at 320 cm^{-1} and the formation of the additional absorption peak. The underlying mechanism, however, is yet unknown and the subject of an ongoing discussion.[1,8,9]

Recently, van der Marel and co-workers have proposed a very interesting explanation for the additional absorption peak.[10,11] They assumed that the CuO_2 planes of the high-T_c cuprate superconductors are not coherently coupled, not even the closely spaced planes of the bilayers. From this point of view a bilayer compound like Y-123 can be treated as a stack of two-dimensional superconducting layers that forms a superlattice of intrabilayer and interbilayer Josephson junctions. The dielectric response of such a superlattice of Josephson junctions exhibits two zero crossings corresponding to two longitudinal Josephson plasmons: the interbilayer and the intrabilayer one. In addition, it has a pole corresponding to the so-called ''transverse optical Josephson plasmon.''[10] Van der Marel and co-workers have suggested that the additional absorption peak discussed above may correspond to this transverse resonance. Very recently they have confirmed their suggestion by more quantitative considerations regarding the doping dependence of the peak position.[11] Some of us have shown that this model can be extended to account not only for the presence of the additional peak but also for the related phonon anomalies.[12] The essential idea consists in including the local electrical fields acting on the ions that participate in the phonon modes. In particular, the model has allowed us to explain the details of the anomaly of the 320-cm^{-1} phonon mode in Y-123. This has been shown to arise from a dramatic change of the local electrical field acting on the in-plane O(2)- and O(3)-ions caused by the onset of interbilayer and intrabilayer Josephson effects.

The verification of the existence of intrabilayer Josephson plasmons may have rather far-reaching consequences. The finding that even the closely spaced CuO_2 layers are only weakly (i.e., Josephson) coupled along the *c*-axis would favor models that predict that the electronic ground state of the CuO_2 planes is unconventional, involving charge confinement to the planes and incoherent coupling between the planes in the normal state.[13] So far, the existence of the Josephson plasma resonance has been firmly established only for the case of CuO_2 planes (or pairs of planes) that are separated by insulating layers much wider than the in-plane lattice constant. Such examples are the studies of the *c*-axis transport,[14,15] the microwave absorption[16] or the far-infrared *c*-axis conductivity.[17–19] Even two different longitudinal plasma modes have been recently observed in the T^* phase $SmLa_{1-x}Sr_xCuO_4$ that has two kinds of blocking layers: the fluorite-type Sm_2O_2 layers and the rocksalt-type $(La,Sr)_2O_2$ layers.[20]

In order to establish the above interpretation of the anomalies in the *c*-axis conductivity of underdoped Y-123, two points have to be clarified that have not been addressed in our previous communication.[12] First, according to the model of the superlattice of interbilayer and intrabilayer Josephson junctions (let us call it a Josephson-superlattice model) the phonon anomalies should become pronounced only below T_c. There may be a gradual onset of the phonon anomalies occurring at temperatures well above T_c due to coherent superconducting correlations which persists within the individual bilayers. Nevertheless, the phonon anomalies should exhibit a sudden increase at T_c when the superconducting state becomes macroscopically coherent. From the previous experimental results it was not clear whether this is the case. Reflectance measurements performed on strongly underdoped Y-123 single crystals rather seemed to indicate that the anomaly of the 320-cm^{-1} phonon sets in well above T_c at a temperature $T^* \gg T_c$ and proceeds without any noticeable change at T_c.[3,9] The temperature dependence of the phonon anomaly rather seemed to resemble[3,21] that of the spin-lattice relaxation rate $(T_1T)^{-1}$ or the Knight shift observed in nuclear magnetic resonance (NMR) experiments, both of which are determined by the so-called ''spin-gap phenomenon,'' i.e., by a gradual and incomplete depletion of the low-energy spin excitations. These speculations are supported by Zn-substitution experiments: the Zn substitution is known to suppress the spin-gap effect[22] and it has also been shown to remove the anomaly of the 320-cm^{-1} phonon mode and the additional absorption peak.[9] Second, the model predicts that the additional peak should acquire a considerable part of its spectral weight from the electronic background, to be more specific, from the superconducting condensate.[12] This prediction is not consistent with Ref. 2 where it has been suggested that the spectral weight of the additional peak is fully accounted for by the spectral-weight loss of the phonon modes at 320 and 560 cm^{-1}.

In the following we report an ellipsometric study of the far-infrared *c*-axis dielectric response of two underdoped $YBa_2Cu_3O_{7-\delta}$ single crystals: one strongly underdoped ($\delta \approx 0.5, T_c = 52$ K), the other moderately underdoped ($\delta \approx 0.25, T_c = 80$ K). In particular, we present a detailed analysis of the anomaly of the oxygen bond-bending mode at 320 cm^{-1} and of the additional absorption peak. In case of the strongly underdoped crystal our ellipsometric measurements establish that the temperature evolution of the phonon anomaly and the additional absorption peak exhibits a two-step behavior with a smooth onset at $T^* \sim 150$ K $\gg T_c = 52$ K followed by a sudden and steep change right at $T_c = 52$ K. For the moderately underdoped crystal the onset of the anomaly occurs in the vicinity of T_c. For both crystals our data establish that the absorption peak obtains only some part of its spectral weight from the phonon system while a substantial part (at least 40%) arises from the electronic background.

II. EXPERIMENTAL TECHNIQUE

A. Sample preparation

The $YBa_2Cu_3O_{7-\delta}$ single crystals with typical dimensions of $2 \times 2 \times (0.5–1)$ mm^3 have been grown in Y-stabilized Zr_2O crucibles.[23] For the ellipsometric measurements we used only crystals with a smooth and shiny as-grown surface containing the *c* axis. A strongly oxygen-deficient crystal has been prepared by sealing it in an evacuated quartz tube together with a large amount of Y-123 powder whose oxygen content has been previously adjusted to $\delta \approx 0.5$ (by annealing in $0.1\% O_2$ in Ar at 530 °C and subsequently quenching into liquid nitrogen). The quartz ampule containing the crystal and the powder was annealed at 500 °C for 10 days and subsequently slowly cooled to room temperature. A second, moderately underdoped $YBa_2Cu_3O_{6.75}$ crystal has been prepared by annealing in a flowing oxygen gas stream at 550 °C and subsequent rapid quenching. The critical temperature T_c and the transition width ΔT_c (10–90 % of the diamagnetic shielding) have been determined by dc-magnetization measurement in zero-

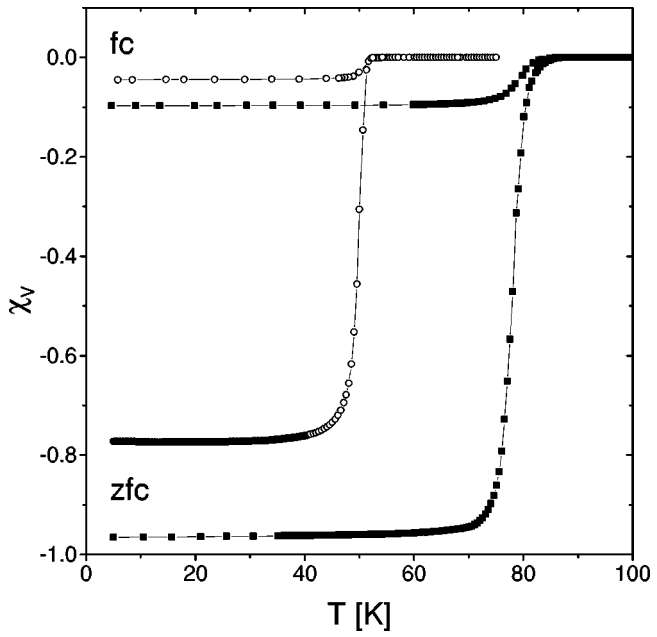

FIG. 1. Temperature dependence of the zero-field-cooled (zfc) and field-cooled (fc) volume dc-magnetization χ_V of the $YBa_2Cu_3O_{6.5}$ crystal (open circles) and the $YBa_2Cu_3O_{6.75}$ crystal (solid squares). The external field $H_{ext}=5$ Oe was applied along the *c* axis of the platelet-shaped crystals. Corrections for demagnetization factors have not been taken into account. The critical temperatures and the transition width (between 10 and 90 % of the diamagnetic shielding) are $T_c=52$ K, $\Delta T_c=3$ K and $T_c=80$ K, $\Delta T_c=4$ K.

field-cooled and field-cooled mode ($H_{ext}=5$ Oe) using a commercial superconducting quantum interference device (SQUID) magnetometer. Figure 1 shows the temperature-dependent volume susceptibility $\varkappa_V$ for the $YBa_2Cu_3O_{6.5}$ crystal with $T_c=52$ K and $\Delta T_c=3$ K (open circles) and the $YBa_2Cu_3O_{6.75}$ crystal with $T_c=80$ K and $\Delta T_c=4$ K (solid squares).

B. Technique of far-infrared ellipsometry

The quantity measured in ellipsometry[24] is the complex reflectance ratio

$$\tilde{\rho}(\omega,\Phi)=\tilde{r}_p(\omega,\Phi)/\tilde{r}_s(\omega,\Phi), \tag{1}$$

where Φ is the angle of incidence (in our experiment 80° with a beam divergence of $\pm 1.2°$) and $\tilde{r}_p$ and $\tilde{r}_s$ are the complex Fresnel reflection coefficients for light that is polarized parallel (*p*) and perpendicular (*s*) to the plane of incidence, respectively. The dielectric function is extracted from $\tilde{\rho}(\omega,\Phi)$ by inverting the Fresnel equations:

$$\tilde{\epsilon}(\omega)=\{[1-\tilde{\rho}(\omega,\Phi)]/[1+\tilde{\rho}(\omega,\Phi)]\}^2\tan^2\Phi\sin^2\Phi + \sin^2\Phi. \tag{2}$$

This inversion assumes an isotropic sample. For an anisotropic sample, in general, different elements of the dielectric tensor can contribute to $\tilde{\rho}(\omega,\Phi)$. The formal inversion according to Eq. (2) then yields only a so-called pseudodielectric function.[25] For the case of $YBa_2Cu_3O_{7-\delta}$, which is an almost uniaxial and strongly anisotropic material with metallic behavior of $\tilde{\epsilon}_{a,b}(\omega)$ and insulating behavior of $\tilde{\epsilon}_c(\omega)$, it was previously shown that the pseudodielectric function represents a very good approximation for $\tilde{\epsilon}_c$ when the measurement is performed with the *c* axis in the plane of incidence.[26]

The technique of ellipsometry provides significant advantages over conventional reflection methods: (i) it does not require the determination of the absolute intensity of the reflected light (no reference problem) and (ii) the complex dielectric function $\tilde{\varepsilon}=\epsilon_1+i\epsilon_2$ is obtained directly, no Kramers-Kronig transformation and thus no extrapolation of the reflectivity towards zero and infinite frequency is needed.[27,28]

The ellipsometric measurements have been performed at the U4IR beamline of the National Synchrotron Light Source (NSLS) at Brookhaven National Laboratory, using a home-built setup attached to a Nicolet Fast-Fourier spectrometer.[27,28] The high brilliance of the synchrotron light source enables us to perform very accurate ellipsometric measurements in the far-infrared range even on samples with comparably small ac faces of 0.5×1 mm^2. Since only relative intensities are required, the ellipsometric measurements are very reproducible and the data taken at a given temperature before and after thermal cycling or several days of measurement coincide to within the noise level.

III. RESULTS

A. Strongly underdoped $YBa_2Cu_3O_{6.5}$

Figure 2 shows the real part of the far-infrared *c*-axis conductivity $\sigma_c(\omega,T)$ of the strongly underdoped $YBa_2Cu_3O_{6.5}$ crystal with $T_c=52$ K for (a) $T=300$, 200, and 150 K and (b) $T=150$, 60, 45, 35 and 4 K. At room temperature the six infrared-active phonon modes at 155, 190, 280, 320, 560, and 630 cm^{-1} are superimposed on a weak and almost featureless electronic background. As the temperature is lowered below room temperature, the electronic background decreases continuously and develops the so-called normal-state gap that is a well-known feature of the underdoped cuprate superconductors.[2,29–32] Evidently, in this strongly underdoped crystal the normal-state gap starts to develop at some rather high temperature, $T^{NG}\gtrsim 300$ K. Its size, which is conveniently defined as the onset frequency ω_{NG} of the suppression of the electronic conductivity with decreasing temperature, is fairly large and it even exceeds the measured spectral range, i.e., $\omega_{NG}>700$ cm^{-1}.[31,32] Figure 2 also shows that the renormalization of the oxygen bond-bending mode at 320 cm^{-1} and the additional broad peak at 410 cm^{-1} exhibit a very gradual onset around $T^*\sim 150$ K, i.e., well below $T_{NG}\gtrsim 300$ K but also well above $T_c=52$ K. However, the most important feature that is evident in Fig. 2(b) is that both the anomaly of the 320 cm^{-1} phonon mode and the formation of the additional absorption peak at 410 cm^{-1}, exhibit very pronounced and steep changes right at $T_c=52$ K. This finding implies that both effects are related to the superconducting transition rather than to the normal-state gap or to the spin-gap phenomenon as has been previously suggested.[3,9] As was mentioned above, the gradual onset of the anomalies at $T^*\gg T_c$ may be explained due to the persistence of a coherent superconduct-

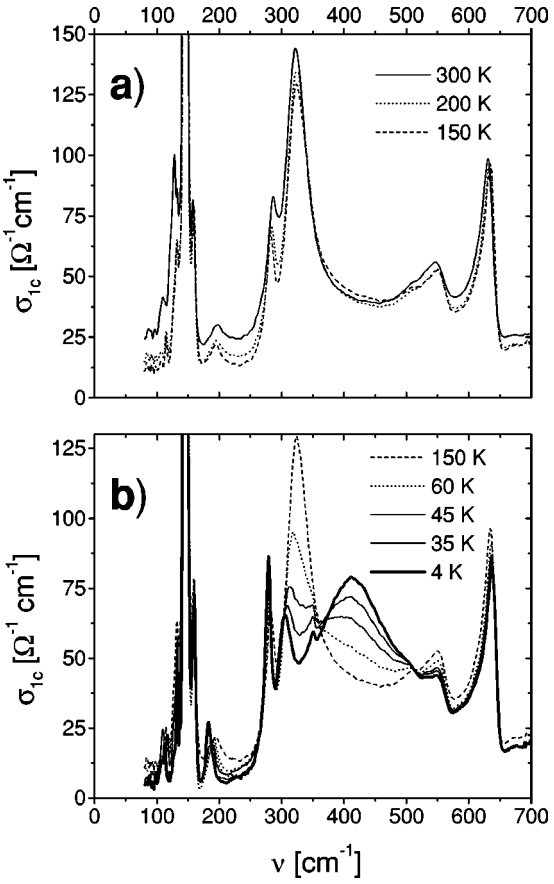

FIG. 2. Temperature dependence of the real part of the far-infrared *c*-axis conductivity of the strongly underdoped $YBa_2Cu_3O_{6.5}$ crystal with $T_c=52$ K. Spectra are shown for (a) $T=300$, 200, and 150 K and (b) T=150, 60, 45, 35, and 5 K.

ing state within the individual bilayers. This effect may become particularly pronounced for the strongly underdoped and thus very anisotropic samples. We do not attempt here to comment on the rather controversial question of whether the normal-state gap and/or the spin gap are also somehow related to superconducting pairing fluctuations.

We have performed a more quantitative data analysis by fitting to the complex dielectric function in the spectral range $250<\omega<700$ cm^{-1} a sum of modified Lorentzian functions $\epsilon(\omega)=S\cdot(\omega_o^2+i\Gamma\cdot Q)/[(\omega_o^2-\omega^2)-i\omega\cdot\Gamma]$ that represent the contributions of the phonon modes at 280, 320, 560, and 630 cm^{-1}. This modified Lorentzian function that is obtained by mixing the real and the imaginary parts of the usual Lorentzian function (it basically corresponds to a Fano-like function) allows one to perform Kramers-Kronig consistent fits of asymmetric phonon lineshapes.[2,3] We find that only the phonon modes at 560 and 630 cm^{-1} are asymmetric and that the asymmetry Q of these modes increases very moderately with decreasing temperature. In order to describe the flat electronic background and the additional broad absorption peak in a Kramers-Kronig consistent way we have also included a sum of seven broad Lorentzian oscillators that have been located between 250 and 700 cm^{-1} and whose half-widths have been limited to values between 150 and 500 cm^{-1}.

In our opinion this fitting procedure does not allow one to obtain an appropriate description of the phonon contribution since it assumes that all the ions participating in the phonon modes experience the same (average) electric field. Instead, as motivated in Ref. 12, we suggested that the local electric fields acting on the ions exhibit significant deviations from the average field as a result of the extremely weak electronic coupling between the individual CuO_2 planes of underdoped cuprates. We have shown that the spectacular anomaly of the 320-cm^{-1} phonon mode, and also the asymmetry and the spectral weight changes of the phonon modes at 560 and 630 cm^{-1}, can be explained by such local field effects, in particular, by the changes of the local electrical fields caused by the onset of Josephson effects within the intrabilayer and interbilayer junctions.[12] In the present paper we nevertheless apply the simpler fitting procedure using modified Lorentzian functions in order to obtain the temperature dependence of the parameters of the phonon modes that can be readily compared with previous results.

Figure 3 shows the temperature dependence of (a) the oscillator strength S, (b) the eigenfrequency ω_o, and (c) the half-width Γ of the oxygen bond-bending mode at 320 cm^{-1}. It is evident from Figs. 3(a) and 3(b) that the changes of S and ω_o set in rather gradually around $T^*\sim150$ K. The temperature dependences of both quantities, however, exhibit a sudden and steep change around $T_c=52$ K. This finding contrasts with previous reports that the renormalization of the 320-cm^{-1} phonon mode does not exhibit any noticeable change around T_c.[3,9] In agreement with the previous reports we find that the half-width Γ of the 320-cm^{-1} mode starts to decrease only below $T_c=52$ K.[1–3,33] For $T^*>T>T_c$ it even tends to increase, but this small increase may be an artifact of our fitting procedure. Figure 4 displays the electronic background including the additional peak around 400 cm^{-1} which has been obtained by subtracting the contributions of the phonon modes at 280, 320, 560, and 630 cm^{-1}. The formation of the additional peak shown in Fig. 4 follows a similar temperature dependence like the anomaly of the 320-cm^{-1} phonon mode. The broad peak gradually develops around $T^*\sim150$ K and suddenly increases in magnitude below $T_c=52$ K. Evidently, the peak position does not change much as a function of temperature. Below T_c the peak is very pronounced and therefore hardly affected by the subtraction of the phononic contribution. The frequency of the maximum decreases slightly from 410 cm^{-1} at 5 K to 395 cm^{-1} at 45 K. Above T_c the peak becomes rather weak as compared to the phonon mode at 320 cm^{-1}. We therefore cannot reliably determine its position. Nevertheless, it is evident that it remains close to 400 cm^{-1}. Note that within the Josephson-superlattice model the peak position is expected to decrease only by about 30 cm^{-1} as the temperature is increased above T_c. The position of the transverse plasmon is determined mainly by the intrabilayer Josephson frequency, which for strongly underdoped samples has been suggested[12] not to exhibit any pronounced changes at T_c since coherent superconducting correlations may be conserved within the individual bilayers even far above the macroscopic critical temperature T_c.

Figure 5 shows a comparison of the temperature dependence of the spectral weight (SW) of the additional 410-cm^{-1} peak SW^{410} (solid squares) with the spectral weight loss of the 320-cm^{-1} phonon mode ΔSW^{320} (open

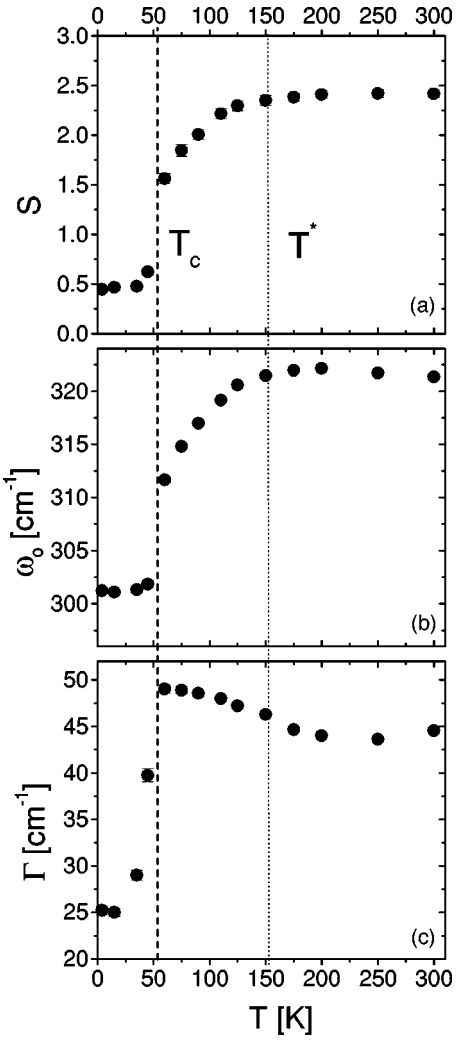

FIG. 3. Temperature dependence of (a) the oscillator strength S, (b) the eigenfrequency ω_o, and (c) the half-width Γ of the oxygen bond-bending mode of the strongly underdoped $YBa_2Cu_3O_{6.5}$ crystal ($T_c=52$ K). The phonon parameters have been obtained by fitting a Lorentzian function to the complex dielectric function. The dashed line marks the superconducting transition temperature $T_c=52$ K, the dotted line indicates the gradual onset of the renormalization of the phonon mode around $T^*\sim 150$ K.

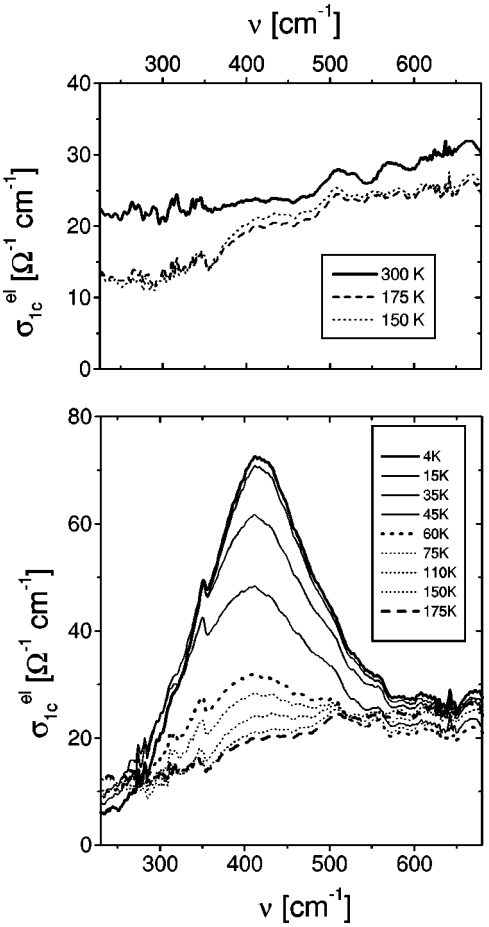

FIG. 4. Temperature dependence of the electronic conductivity including the additional absorption peak at 410 cm^{-1} (presumed to be also of electronic origin) of the strongly underdoped $YBa_2Cu_3O_{6.5}$ crystal with $T_c=52$ K which has been obtained by subtracting the contributions of the phonon modes at 280, 320, 560, and 630 cm^{-1}.

circles). The value of ΔSW^{320} has been calculated according to the formula $\Delta SW=\pi^2 c\cdot\epsilon_o\cdot[S(175\ \mathrm{K})-S(T)]\cdot\nu_o^2$ using the oscillator strength $S(T)$ and the eigenfrequencies ν_o given in Figs. 3(a) and 3(b). The error bar indicates the upper limit for the spectral weight losses of the apical oxygen modes at 560 and 630 cm^{-1}. The inset of Fig. 5 illustrates how we have estimated the spectral weight of the additional peak SW^{410} (shaded area) by integrating the conductivity between 220 and 680 cm^{-1} (open circles) and subtracting the contribution of a linear electronic background (solid line). Note that our assumption of a linear-electronic-background conductivity is supported by the high-temperature data for $T>T^*=150$ K [see Fig. 4(a)] and by the data for less strongly underdoped samples where the additional peak is comparably weak and appears only below T_c (see Refs. 31,32 and discussion below). It is evident from Fig. 5 that the spectral-weight losses of the phonon modes at 320 and 560 cm^{-1} account only for some fraction of the spectral weight of the additional absorption peak at 410 cm^{-1}. We estimate that at least 40% of the spectral weight of the additional absorption peak does not arise from the phonon subsystem but instead seems to arise from the electronic continuum. Such a redistribution of the electronic spectral weight towards the additional absorption peak is predicted by the Josephson-superlattice model where the transverse Josephson plasmon acquires a sizeable fraction of the spectral weight of the SC condensate.[11,12] This means that some fraction of the spectral weight that is removed in the far-infrared regime does not appear in the δ function at zero frequency that describes the inductive response of the superfluid condensate but is instead shifted to the additional absorption peak representing the transverse Josephson plasmon. In fact, our choice of the linear electronic background (solid line) is rather conservative. Also shown in the inset is a fit with a Lorentzian plus a linear electronic background conductivity (dashed lines) that gives a somewhat larger value of $SW^{410}\approx 16\,000\ \Omega^{-1}\,\mathrm{cm}^{-2}$ at $T=5$ K. The result of this fit agrees surprisingly well with the prediction of the Josephson-superlattice model that the spectral weight of the bare transverse Josephson plasmon [neglecting the interaction with the phonons and the consequent redistribution of the spectral

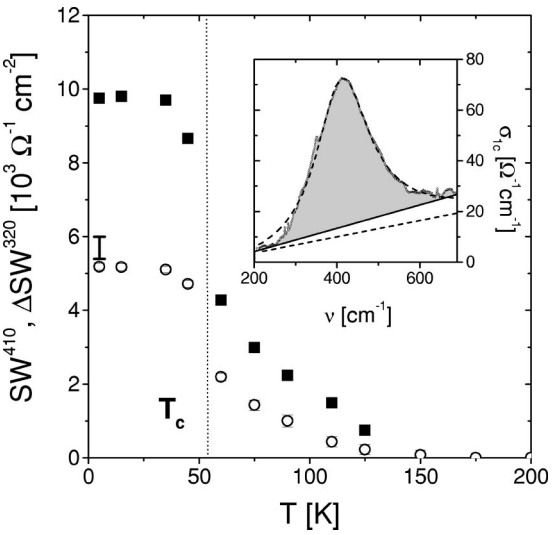

FIG. 5. Temperature dependence of the spectral weight of the additional absorption peak at 410 cm^{-1}(SW^{410}, solid squares) and the spectral-weight loss of the oxygen bond-bending mode at 320 cm^{-1} (ΔSW^{320}, open circles). The inset illustrates how the SW of the additional absorption peak has been obtained. The open circles represent the spectrum at $T=5$ K obtained after the phonons have been subtracted, the solid line represents the linear background that has been further subtracted in order to obtain SW^{410} as indicated by the shaded area. Also shown is a fit with a Lorentzian plus a linear background (dashed lines) that gives a somewhat larger value of $SW^{410}\approx 16\,000\ \Omega^{-1}\,cm^{-2}$ at 5 K. The spectral-weight loss of the 320-cm^{-1} phonon mode has been calculated according to the formula $\Delta SW^{320}=\pi^2 c\cdot\epsilon_o\cdot[S(175\ \mathrm{K})-S(T)]\cdot\nu_o^2$ using the oscillator strength $S(T)$ and the eigenfrequencies ν_o given in Figs. 3(a) and 3(b). The error bar indicates the maximum spectral-weight losses at $T=5$ K of the phonon modes at 560 and 630 cm^{-1}.

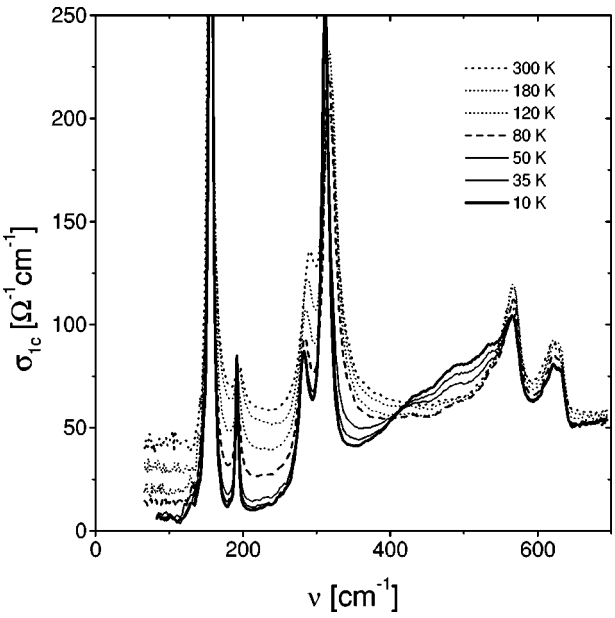

FIG. 6. Temperature dependence of the real part of the far-infrared c-axis conductivity of the weakly underdoped $YBa_2Cu_3O_{6.75}$ crystal with $T_c=80$ K.

weight of the 320-cm^{-1} phonon mode, $\Delta SW^{320}(5\ \mathrm{K})\approx 5000\ \Omega^{-1}\,cm^{-2}$] should be around 10 000 $\Omega^{-1}cm^{-2}$[12].

It has been reported previously that the spectral weight of the additional absorption peak can be fully accounted for by the spectral-weight loss of the phonon modes at 320 and 560 cm^{-1}.[2] We note that this discrepancy between the conclusions of Ref. 2 and of ours does not arise from any significant differences in the experimental data but rather originates from the difference in the estimate of the electronic background. In Ref. 2 the spectral weight of the additional absorption peak seems lower since an electronic background has been introduced that develops a gaplike feature around 280 cm^{-1} (see, for example, Fig. 10 of Ref. 2). It was argued that this gap feature is related to the normal-state gap. Our recent ellipsometric data, however, do not support this interpretation because they show that the size of the normal-state gap ω_{NG} (as defined by the onset frequency of the suppression of the electronic conductivity with decreasing temperature) is significantly larger: it increases from $\omega_{NG}\approx 650$ cm^{-1} for slightly underdoped samples to $\omega_{NG}\gg 700$ cm^{-1} for strongly underdoped samples.[31,32] We have also shown that the temperature at which the signatures of the normal-state gap start to appear increases rather rapidly on the underdoped side and even exceeds room temperature for strongly underdoped samples (see also Fig. 2). Note that recent ARPES and tunneling experiments yield a similar temperature and doping dependence of the normal-state gap (even the absolute values of its size are in good agreement).[34–37] It therefore appears that the additional absorption peak and the normal-state gap have rather different energy and temperature scales. Also, as shown below, they have an opposite doping dependence. Altogether, these findings make it rather unlikely that both phenomena have a common origin.

B. Moderately underdoped $YBa_2Cu_3O_{6.75}$

We have also performed far-infrared ellipsometric measurements on a less strongly underdoped $YBa_2Cu_3O_{6.75}$ sample with $T_c=80$ K. Figure 6 shows its c-axis conductivity $\sigma_c(\omega,\mathrm{T})$ at different temperatures between 300 and 10 K. The anomaly of the oxygen bond-bending mode at 320 cm^{-1} is significantly weaker than that of the strongly underdoped sample. The additional absorption peak is located at higher frequencies (around 480 cm^{-1}) and it is less pronounced. Figure 7 shows the temperature dependence of (a) the oscillator strength S, (b) the eigenfrequency ω_o, and (c) the half-width Γ of the 320-cm^{-1} phonon mode that have been obtained using the fitting procedure outlined above. It can be seen that the onset of the anomaly of the 320-cm^{-1} mode occurs now very close to the superconducting transition (i.e., $T^*\lesssim 100$ K). A similar result has been previously obtained from conventional reflection measurements on weakly underdoped Y-123 crystals.[3] Once more the formation of the normal-state gap, as evidenced from the gradual suppression of the electronic background conductivity, sets in at a significantly higher temperature $T_{NG}\gtrsim 200$ K. The size of the normal-state gap has decreased to $\omega_{NG}\sim 700$ cm^{-1}. As was outlined above, these findings lead us to conclude that the anomaly of the 320-cm^{-1} mode and the formation of the additional absorption peak are not directly related to the mechanism that is underlying the normal-state

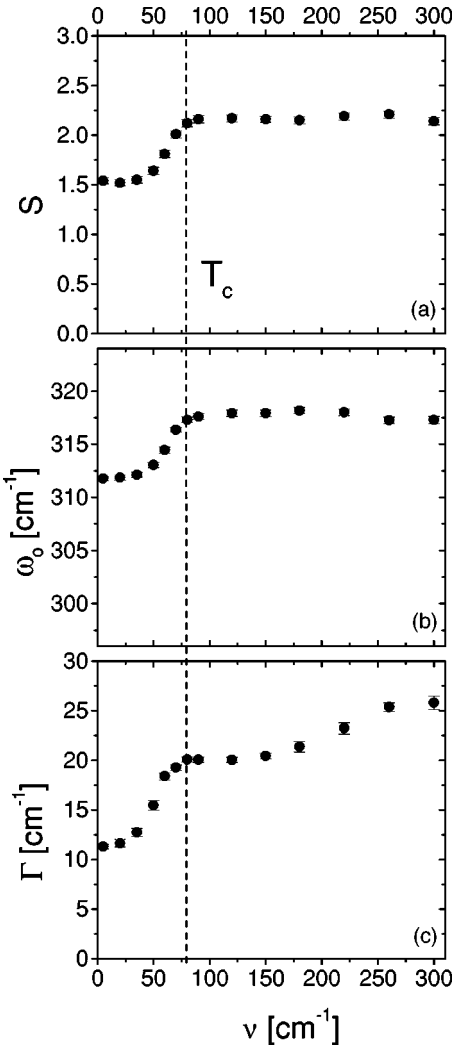

FIG. 7. Temperature dependence of (a) the oscillator strength S, (b) the eigenfrequency ω_o, and (c) the half-width Γ of the oxygen bond-bending mode of the moderately underdoped $YBa_2Cu_3O_{6.75}$ crystal ($T_c = 80$ K). The phonon parameters have been obtained by fitting a Lorentzian function to the complex dielectric function. The dashed line marks the superconducting transition temperature $T_c = 80$ K.

gap.[31,32] Figure 8 shows the electronic background including the additional absorption peak that has been obtained by subtracting the contributions of the phonon modes at 280, 320, 570, and 620 cm^{-1} (as described above). Figure 9 shows the estimated temperature dependences of the spectral weight of the additional peak at 480 cm^{-1} (once more assuming a linear electronic background) and of the spectral weight loss of the phonon mode at 320 as estimated from the change of its oscillator strength according to $\Delta SW^{320} = \pi^2 c \cdot \epsilon_o \cdot [S(120\ \mathrm{K}) - S(T)] \cdot \nu_o^2$. In analogy to the strongly underdoped sample, a sizeable fraction of the spectral weight of the absorption peak does not seem to arise from the phonon subsystem.

IV. SUMMARY

In summary, we have performed ellipsometric measurements of the far-infrared *c*-axis conductivity of underdoped $YBa_2Cu_3O_{7-\delta}$ single crystals. In particular, we have studied

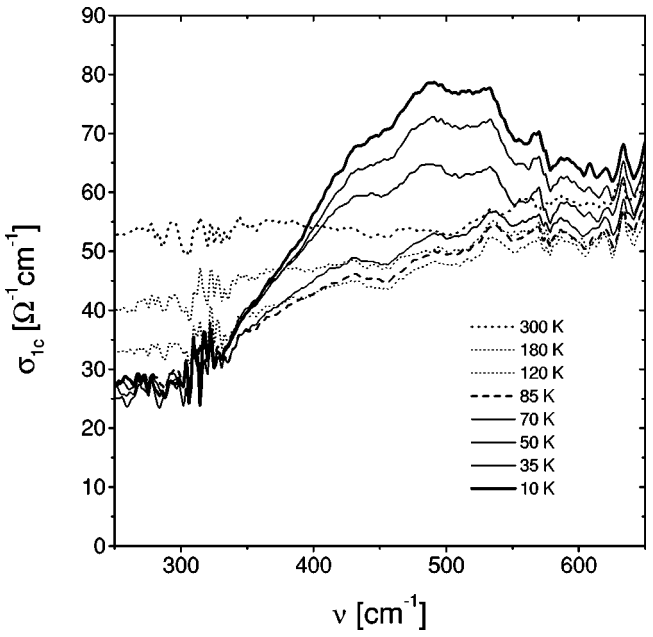

FIG. 8. Temperature dependence of the electronic conductivity, including the additional absorption peak around 480 cm^{-1}, of the moderately underdoped $YBa_2Cu_3O_{6.75}$ crystal with $T_c = 80$ K that has been obtained by subtracting the contributions of the phonon modes at 280, 320, 570, and 620 cm^{-1}.

the temperature dependence of the spectacular anomaly of the oxygen bond-bending mode at 320 cm^{-1} and of the additional absorption peak. For the strongly underdoped $YBa_2Cu_3O_{6.5}$ crystal with $T_c = 52$ K the gradual onset of the anomaly of the 320-cm^{-1} phonon mode and the growth of the additional absorption peak around 410 cm^{-1} occur

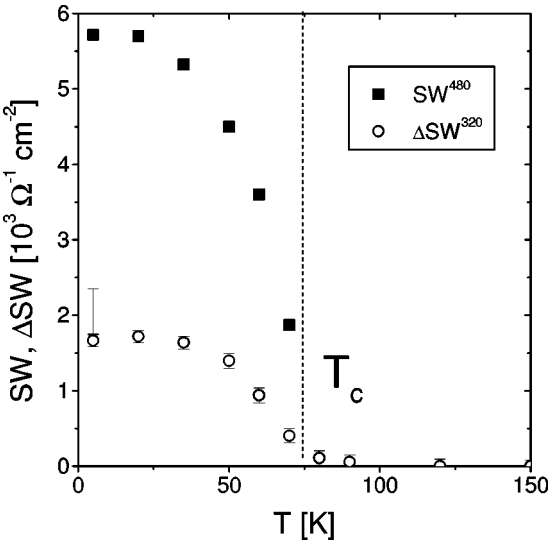

FIG. 9. Temperature dependence of the spectral weight of the additional absorption peak at 480 cm^{-1}(SW^{480}, solid squares) and the spectral weight loss of the oxygen bond-bending mode at 320 cm^{-1}(ΔSW^{320}, open circles). The spectral-weight loss of the 320-cm^{-1} phonon mode has been calculated according to the formula $\Delta SW = \pi^2 c \cdot \epsilon_o \cdot [S(120\ \mathrm{K}) - S(T)] \cdot \nu_o^2$, using the oscillator strengths $S(T)$ and the eigenfrequencies ν_o given in Figs. 7(a) and 7(b). The error bar indicates the maximum spectral-weight losses at $T = 5$ K of the phonon modes at 570 and 630 cm^{-1}.

around $T^* \sim 150$ K, i.e., well below the onset temperature of the normal-state gap $T_{NG} \gtrsim 300$ K, but also well above $T_c = 52$ K. Most remarkably, however, we find that both anomalies exhibit a very pronounced and marked change right at $T_c = 52$ K. For a less strongly underdoped $YBa_2Cu_3O_{6.75}$ crystal with $T_c = 80$ K both anomalies start to appear in the vicinity of the superconducting transition, $T^* \sim T_c = 80$ K while the signatures of the normal-state gap appear below $T_{NG} \gtrsim 200$ K. Our measurements thus establish that both anomalies are related to the superconducting transition. For strongly underdoped and thus very anisotropic samples, the gradual onset of the anomalies may occur well above T_c due to the persistence of a coherent superconducting state within the individual bilayers, but there is always a steep and sudden increase of both anomalies when the macroscopically coherent superconducting state forms at T_c. This implies that the anomalies are not related to the normal-state gap in the *c*-axis conductivity nor to the spin-gap phenomenon as observed in NMR and nuclear quadrupole resonance measurements both of which exhibit no noticeable change at T_c. For both underdoped crystals a sum-rule analysis of the changes of the spectral weights indicates that the spectral weight of the additional absorption peak is not fully accounted for by the spectral-weight loss of the phonon modes at 320 and 560 cm^{-1}. At least 40% of the spectral weight of the additional absorption peak seems to arise from the electronic background, namely from the superconducting condensate. We have outlined that all the reported features are compatible with a recently proposed model where the bilayer cuprate compounds such as Y-123 are treated as a superlattice of interbilayer and intrabilayer Josephson junctions. The additional absorption peak can be related to the transverse optical plasmon, while the spectacular phonon anomaly can be explained as due to the drastic changes of the local electrical fields acting on the in-plane oxygen ions as the Josephson current sets in below T_c for the interbilayer junctions while below $T^* \geqslant T_c$ for the intrabilayer junctions.

ACKNOWLEDGMENTS

We gratefully acknowledge the support of G.P. Williams and L. Carr at the U4IR beamline at NSLS. We also thank D. Böhme and W. König for technical help and E. Brücher and R.K. Kremer for performing the SQUID measurements. D.M. gratefully acknowledges support by the Alexander von Humboldt Foundation.

*Permanent address: IFD, Warsaw University, Hoza 69, 00-681 Warsaw, Poland.

[1] A. Wittlin, R. Liu, M. Cardona, L. Genzel, W. König, and F. Garcia-Alvarado, Solid State Commun. **64**, 477 (1987); A.P. Litvinchuk, C. Thomsen, and M. Cardona, in *Physical Properties of High Temperature Superconductors IV*, edited by D.M. Ginsberg (World Scientific, Singapore, 1994), p. 375 and references therein.

[2] C.C. Homes, T. Timusk, D.A. Bonn, R. Liang, and W.N. Hardy, Physica C **254**, 265 (1995); Can. J. Phys. **73**, 663 (1995).

[3] J. Schützmann, S. Tajima, S. Miyamoto, Y. Sato, and R. Hauff, Phys. Rev. B **52**, 13 665 (1995).

[4] D.N. Basov, T. Timusk, B. Dábrowski, and J.D. Jorgensen, Phys. Rev. B **50**, 3511 (1994).

[5] M. Reedyk, T. Timusk, Y.W. Hsueh, B.W. Statt, J.S. Xue, and J.E. Greedan, Phys. Rev. B **56**, 9129 (1997).

[6] T. Zetterer, M. Franz, J. Schützmann, W. Ose, H.H. Otto, and K.F. Renk, Phys. Rev. B **41**, 9499 (1990).

[7] R. Henn, T. Strach, E. Schönherr, and M. Cardona, Phys. Rev. B **55**, 3285 (1997).

[8] G. Hastreiter, U. Hoffmann, J. Keller, and K.F. Renk, Solid State Commun. **76**, 1015 (1990).

[9] R. Hauff, S. Tajima, W.J. Jang, and A.I. Rykov, Phys. Rev. Lett. **77**, 4620 (1996).

[10] D. van der Marel and A.A. Tsvetkov, Czech. J. Phys. **46**, 3165 (1996).

[11] M. Grüninger, D. van der Marel, A.A. Tsvetkov, and A. Erb, cond-mat/9903352 (unpublished).

[12] D. Munzar, C. Bernhard, A. Golnik, J. Humlíček, and M. Cardona, Solid State Commun. **112**, 365 (1999).

[13] P.W. Anderson, *The Theory of Superconductivity in the High-T_c Cuprates* (Princeton University Press, Princeton, NJ, 1997).

[14] M. Rapp, A. Murk, R. Semerad, and W. Prusseit, Phys. Rev. Lett. **77**, 928 (1996).

[15] K. Schlenga, R. Kleiner, G. Hechtfischer, M. Mößle, S. Schmidt, P. Müller, Ch. Helm, Ch. Preis, F. Forsthofer, J. Keller, H.L. Johnson, M. Veith, and E. Steinbeiß, Phys. Rev. B **57**, 14 518 (1998).

[16] Y. Matsuda, M.B. Gaifullin, K. Kumagai, K. Kadowaki, and T. Mochiku, Phys. Rev. Lett. **75**, 4512 (1995); O.K.C. Tsui, N.P. Ong, and J.B. Petterson, *ibid.* **76**, 819 (1996).

[17] K. Tamasaku, T. Ito, H. Takagi, and S. Uchida, Phys. Rev. Lett. **72**, 3088 (1994).

[18] P.J.M. van Bentum, A.M. Gerrits, M.E. Boonamn, A. Wittlin, V.H.M. Dujin, and A.A. Menovski, Physica B **211**, 260 (1995).

[19] P.J.M. van Bentum, A. Wittlin, M.E.J. Boonman, M. Gross, S. Uchida, and K. Tamasaku, Physica C **293**, 136 (1997).

[20] H. Shibata and T. Yamada, Phys. Rev. Lett. **81**, 3519 (1998).

[21] A.P. Litvinchuk, C. Thomsen, M. Cardona, J. Karpinski, E. Kaldis, and S. Rusiecki, Z. Phys. B: Condens. Matter **92**, 9 (1993).

[22] See, for example, K. Kakurai, S. Shamoto, T. Kiyokura, M. Sato, J.M. Tranquada, and G. Shirane, Phys. Rev. B **48**, 3485 (1993); G.V.M. Williams, J.L. Tallon, R. Meinhold, and A. Janossy, *ibid.* **51**, 16 503 (1995).

[23] C.T. Lin, W. Zhou, W.Y. Liang, E. Schönherr, and H. Bender, Physica C **195**, 291 (1992).

[24] R.M.A. Azzam and N.H. Bashara, *Ellipsometry and Polarized Light* (North-Holland, Amsterdam, 1977).

[25] D.E. Aspnes, J. Opt. Soc. Am. **70**, 1275 (1980).

[26] R. Henn, J. Kircher, M. Cardona, A. Wittlin, V.H.M. Dujin, and A.A. Menovsky, Phys. Rev. B **53**, 9353 (1996).

[27] J. Kircher, R. Henn, M. Cardona, P.L. Richards, and G.P. Williams, J. Opt. Soc. Am. B **14**, 705 (1997).

[28] R. Henn, C. Bernhard, A. Wittlin, M. Cardona, and S. Uchida, Thin Solid Films **313-314**, 643 (1998).

[29] S. Tajima, J. Schützmann, S. Miyamoto, I. Terasaki, Y. Sato, and R. Hauff, Phys. Rev. B **52**, 13 665 (1997).

[30] C. Bernhard, R. Henn, A. Wittlin, M. Kläser, Th. Wolf, G. Müller-Vogt, C.T. Lin, and M. Cardona, Phys. Rev. Lett. **80**, 1762 (1998).

[31] C. Bernhard, D. Munzar, A. Wittlin, W. König, A. Golnik, C.T. Lin, M. Kläser, Th. Wolf, G. Müller-Vogt, and M. Cardona, Phys. Rev. B **59**, R6631 (1999).

[32] C. Bernhard, D. Munzar, A. Golnik, M. Kläser, Th. Wolf, C.T. Lin, and M. Cardona, Physica C **317-318**, 276 (1999).

[33] A.P. Litvinchuk, C. Thomsen, and M. Cardona, Solid State Commun. **83**, 343 (1992).

[34] H. Ding, M.R. Norman, T. Yokoya, T. Takeuchi, M. Randeira, J.C. Campuzano, T. Takahashi, T. Mochiku, and K. Kadowaki, Phys. Rev. Lett. **78**, 2628 (1997); Nature (London) **382**, 51 (1996).

[35] A.G. Loeser, Z.-X. Shen, D.S. Dessau, D.S. Marshall, C.H. Park, P. Fournier, and A. Kapitulnik, Science **273**, 325 (1996).

[36] M.R. Norman, H. Ding, M. Randeira, J.C. Campuzano, T. Yokoya, T. Takeuchi, T. Takahashi, T. Mochuki, K. Kadowaki, P. Guptasarama, and D.G. Hinks, Phys. Rev. B **57**, 11 093 (1998); Nature (London) **392**, 157 (1998).

[37] N. Miyakawa, P. Guptasarma, J.F. Zsadzinski, D.G. Hinks, and K.E. Gray, Phys. Rev. Lett. **80**, 157 (1998).